UNIVERSITY OF BATH

Citation for published version:
Lebekwe, CK, Zungeru, AM & Astin, I 2021, 'Meteorological Influence on eLoran Accuracy', *IEEE Access*, vol. 9, pp. 167162 - 167172. https://doi.org/10.1109/ACCESS.2021.3135707

DOI:
10.1109/ACCESS.2021.3135707

Publication date:
2021

Document Version
Publisher's PDF, also known as Version of record

Link to publication

Publisher Rights
CC BY

University of Bath

Alternative formats
If you require this document in an alternative format, please contact:
openaccess@bath.ac.uk

General rights
Copyright and moral rights for the publications made accessible in the public portal are retained by the authors and/or other copyright owners and it is a condition of accessing publications that users recognise and abide by the legal requirements associated with these rights.

Take down policy
If you believe that this document breaches copyright please contact us providing details, and we will remove access to the work immediately and investigate your claim.

Download date: 05. May. 2023

This article has been accepted for publication in a future issue of this journal, but has not been fully edited. Content may change prior to final publication. Citation information: DOI 10.1109/ACCESS.2021.3135707, IEEE Access

IEEE Access
Multidisciplinary | Rapid Review | Open Access Journal

Date of publication xxxx 00, 0000, date of current version xxxx 00, 0000.

Digital Object Identifier 10.1109/ACCESS.2017.DOI

Meteorological Influence on eLoran Accuracy

CASPAR K. LEBEKWE, MEMBER, IEEE[1], ADAMU MURTALA ZUNGERU, SENIOR MEMBER, IEEE[1], AND IVAN ASTIN, MEMBER, IEEE[2]

[1]Department of Electrical, Computer and Telecommunications Engineering, Botswana International University of Science and Technology, Botswana
[2]Department of Electronic and Electrical Engineering, University of Bath, United Kingdom

Corresponding authors: Caspar K. Lebekwe; Adamu Murtala Zungeru (e-mail: lebekwec@biust.ac.bw;zungerum@biust.ac.bw).

This work was supported in part by the Botswana International University of Science and Technology (BIUST) Department of Electrical, Computer and Telecommunications Engineering.

ABSTRACT Stringent accuracy requirements need to be met for eLoran deployment in marine navigation and harbour entrance and approach. A good accuracy model is therefore required to predict the positioning accuracy at the user's receiver locations. Accuracy depends on the variations of additional secondary factors (ASFs) and the primary factor delay. The changes in the air refractive index caused variations in the primary factor (PF) delay of the eLoran signal, and current eLoran accuracy models do not take this into account. This paper proposes an improved empirical accuracy model that considers the contributions of changes in the refractive index of the air, often classified as a short term effect. The changes in weather parameters such as atmospheric pressure and temperature increase the time of arrival variance. The developed accuracy model is used to predict the eLoran positioning error in the European maritime region. The results show that the short term ASF variations significantly contribute to the positioning error and must be included in the accuracy model. The results also demonstrate that a 20 m accuracy or better would be achieved in the North Sea, while a 10 m accuracy would be achievable at the SOLAS ports if eLoran was reintroduced in Europe. Nevertheless, the repeatable accuracy around the Irish sea exceeds 80 m and does not meet marine navigation requirements compared to GPS. Coverage can be enhanced by including at least two eLoran transmitters in Ireland.

INDEX TERMS eLoran, refractive index, Temporal ASFs, Accuracy

I. INTRODUCTION

The United States Global Positioning System (GPS) has for decades become an essential part of society. It has been established as the primary source of position, navigation and timing (PNT) information for land, air and sea. While it has superior qualities that make it more appealing than its rivals, the strength of GPS signals, especially at the Earth surface, have been documented to be extremely low [1]. This Achilles heel is present in all Global Navigation Satellite Systems (GNSS) and poses economic, safety and environmental risks associated with over-reliance on a single satellite navigation system. This view was included in the report [33] prepared for the United States Department of Transport. A Low Frequency (LF) terrestrial system, a redundant system with different failure modalities called LOng RAnge Navigation (LORAN) system, was chosen as a suitable backup. It was pointed out that Loran, in its form, cannot meet the stringent standards set by the governing bodies. In 2004, U.S. Federal Aviation Administration (FAA) issued a report confirming eLoran as a suitable backup for GNSS systems. eLoran is designed to serve as a stand-alone and back up to GPS [1]. In 2006, The U.S. Department of Homeland Security and the Department of Transportation funded the Institute for Defense Analyses to form an Independent Assessment Team (IAT) to review the need for an eLoran system as a backup to GPS. The IAT unanimously recommended an upgrade of all Loran systems and that eLoran must be a national GPS backup for 20 years [31]. All eLoran applications must meet the standard set by the IMO [18].

The General Light House Authorities of the United Kingdom and Ireland (GLA) was awarded a 15-year contract [34], but sadly, at the end of 2015, the European eLoran transmitters were shut down following the decision by the nations hosting the transmitters to cease to fund eLoran transmission. Nevertheless, eLoran deployment in Korea is still ongoing. The general eLoran system operations are

This work is licensed under a Creative Commons Attribution 4.0 License. For more information, see https://creativecommons.org/licenses/by/4.0/

This article has been accepted for publication in a future issue of this journal, but has not been fully edited. Content may change prior to final publication. Citation information: DOI 10.1109/ACCESS.2021.3135707, IEEE Access

described extensively in [1]–[4]. Several types of eLoran stated in the eLoran definition document [6] are aviation non-precision instrument Approaches (NPA), maritime Harbour Entrance and Approach (HEA) manoeuvres, land-mobile vehicle navigation, and location-based services, each with different performance specifications for the four system parameters. These parameters are accuracy, availability, integrity, and continuity. The definition of these parameters are stated in [6], [7], [11].

This work focuses on eLoran for maritime Harbour Entrance and Approach (HEA) manoeuvres where repeatable accuracy is critical. Factors affecting eLoran performance during HEA manoeuvres must be identified and their contributions quantified. These factors are often categorised into long and short term effects and are listed in [23]. The long term effects include seasonal changes in ground conductivity due to rain soaking into the earth, passing weather fronts as well as freeze and thaw of the terrain over which the signals propagate [14]. These lead to signal delay called additional secondary factor (ASF) that varies over time in a stochastic manner.

The short terms effects are mostly due to changes in the meteorological parameters such as temperature, atmospheric pressure, humidity, soil moisture content, and salinity [25]. Even though weather changes affect the primary factor (PF) delay, this PF delay change is normally considered a change in ASF by the eLoran receiver. ASF variations are monitored using a differential Loran (dLoran) set up described in [6], [9]–[11], [14], [20], [22]. By design, system analysts assume that the temporal ASF variations monitored by the dLoran system are the same as those at the user's receiver location. The manifestation of these hazards on accuracy can be mitigated at only port locations but remain prominent elsewhere and are unmitigated due to limited dLoran resources. It is important to note that temporal ASF variations translate to the temporal variation of the position solution. Therefore monitoring and mitigating these variations improves the stability of the position solution.

A. CONTRIBUTIONS

This paper is a continuation of the previous work done by the authors [20] and now adds the contribution of the changes in meteorological parameters on the transmitter ranging errors experienced at the mariner's location. This result in an improved and realistic accuracy prediction model for harbour entrance approaches (HEA). The work in previous studies assumed that a significant contribution to the eLoran accuracy could be attributed to the long-term temporal variations in the times-of-arrival (TOAs) of Loran signals while ignoring the short term effects contributions. The authors in [22] stated that pseudo-range errors experienced at the receiver's position are in the short term caused by the changes in atmospheric parameters along the transmitter-receiver propagation path. The inclusion of the contribution of the atmospheric parameters results in poor repeatable accuracy values in regions where there is no DeLoran.

Therefore, including the contribution of the meteorological parameters in the TOA variance model gives a realistic estimate of the repeatable accuracy performance in a coverage area. Position accuracy is assessed to determine if it meets the performance standard set by the IMO. In summary, the contributions of this research are as follows

- The effects of long-term ASF variations are included in the accuracy model
- Models the impact of the short term ASF variations and includes this in the accuracy model to depict accuracy performance in areas not designated as reference stations
- Applies the long term and short term accuracy models at regions not designated as reference stations. The models in the literature assume that all areas host a reference station.
- Overall, the proposed accuracy model is more realistic and represents what happens in an eLoran operated coverage area than the models seen in the literature.

This article is divided into five sections. Section II describes the improved accuracy model. The model parameters for the contributions of meteorological parameters on the transmitter's pseudo-range error measured at the receiver's location are derived in section III. Section IV discusses the results, while Section V concludes the article.

II. RELATED WORKS

Loran based coverage prediction using repeatable accuracy started in the early 1990s in Europe. Table 1 summaries the findings of several works that studied the hazards that introduce position errors and repeatable accuracy models.

A. EXISTING ACCURACY MODELS

This section describes existing accuracy models found in the literature. Repeatable accuracy describes how stable the measured position is overtime [19]. It represents the scatter of the user's static position and is determined assuming that the uncertainty in the phase measurements is the same. Authors of [15], [20], [23] described the factors that contribute to phase measurement uncertainty. The atmospheric noise measured at the front-end of the receiver influences the signal to noise ratio (SNR) and the residual number of pulses left after application of CRI mitigation procedures [17]. The eLoran position accuracy follows the procedure described in [5], [7], [17], [20], [29].

1) INFLUENCE OF GRI AND SNR ON RANGING ERRORS

This section describes the influence of group repetition interval (GRI), Cross rate Interference (CRI) and SNR on ranging errors. The accuracy model described in [5], [7], [16], [17] are employed by assuming that there is differential Loran (dLoran) everywhere in the coverage area. The TOA variance for any transmitted eLoran signal measured at the user's receiver is given by

This work is licensed under a Creative Commons Attribution 4.0 License. For more information, see https://creativecommons.org/licenses/by/4.0/

This article has been accepted for publication in a future issue of this journal, but has not been fully edited. Content may change prior to final publication. Citation information: DOI 10.1109/ACCESS.2021.3135707, IEEE Access

TABLE 1: eLoran and Loran repeatable accuracy articles

Source	Summary	Year	Citations
[25]	The researchers of this work demonstrated the disparity of the meteorological parameters at various points along the propagation path. They argued that using values of meteorological parameters measured at a single point, as is the practice case, is inaccurate, especially at the receiver position to represent the overall meteorological changes along the propagation path. Their proposed method, called generalized regression neural network (GRNN), better predicts the TOA delay.	2021	2
[26]	Hargreaves et al. gave a general overview of the capabilities of the coverage software developed for the General Light House Authorities. The paper described the spatial decorrelation contribution to the ranging error at the user as being equal to the 10% of the corrected ASF. The TOA variance model also included the contribution of the skywave ground ratio to the ranging errors. .	2015	1
[7]	The authors of this article proposed two things: an eLoran SNR definition and blanking techniques to mitigate the effects of atmospheric noise on eLoran repeatable accuracy over the British Isles. This TOA variance model resulted in an improved eLoran repeatable accuracy compared to the one used in [2]	2011	8
[31]	The authors of this work assessed the temporal ASF models for eLoran in aviation application. They also examined the performance of the model bounds on the pseudo ranges and how they translate into the achieved position errors. This work responded to the task given to the Loran Integrity panel assigned by the FAA to determine if eLoran can be a suitable backup candidate to GPS.	2008	11
[19]	This paper proposed receiver signal processing techniques for mitigating the effects of carrier wave interference which was prevalent at that time	1993	32
[6]	Boyce investigated the impact of atmospheric noise on position accuracy and proposed techniques to mitigate its impact	2007	14
[17]	Safar investigated the effects of cross-rate interference inside eLoran receivers and proposed the mitigation techniques to improve repeatable accuracy	2014	12
[12]	The authors investigated the accuracy mismatch obtained when using ASF corrections from nearby monitor sites. The goal was to assess if corrections from different nearby sites could be interpolated in order to achieve the stipulated accuracy requirements	2008	3
[28]	Johnson et al. proposed a signal of opportunity (SoOP) approach similar to IoT as an alternative to GNSS. Here various technological solutions such as MF DGNSS, AIS and eLoran are used to offer ranging mode (R-mode) to obtain position solution using a mixture of these signals	2014	0
[27]	The authors stated that the ASF exhibits diurnal variation with temperature and rainfall of 30ns and 100ns, respectively. These are equivalent to 9m and 30m.	2017	0

$$\sigma_{TX}^2 = \frac{337.5^2}{N_a\gamma} + \frac{b_1}{N_a} + b_2. \tag{1}$$

where N_a is the number of averaged pulses, b_1 is the transmitter jitter, b_2 represents other unknown sources of error, and γ represents the SNR of each transmitter in view at the user's location. Sherman Lo et al. [16] employed equation (1) in their Loran coverage prediction . Safar et al. [7] proposed that the TOA variance is given by

$$\sigma_{TX}^2 = L_m \frac{337.5^2}{N_a\gamma} \tag{2}$$

where L_m is the inbuilt losses of the receiver under study.

$$N_a = (1 - L_b)\frac{8 \times 10^5}{GRI}. \tag{3}$$

where L_b represents the pulses that remain after blanking and GRI is the group repetition interval. Equation (2) can be verified using the maximum likelihood estimation technique.

2) INFLUENCE OF SKYWAVE ON RANGING ERRORS

The authors in [35] studied the skywave influence on ranging errors and considered it as a threat and hazard to the safety and position accuracy of a navigation system. The ranging error introduced is modelled as a function of the skywave-groundwave ratio [26], [29] The work in [36] proposed a high precision method that can be employed in the receiver frontend to separate skywave occurring as early as 35μ s from groundwave under low SNR conditions.

While the described models presented a significant leap in progress towards modelling repeatable accuracy, it is essential to note that many authors modelled repeatable accuracy under the assumption that dLoran is deployed everywhere in

This work is licensed under a Creative Commons Attribution 4.0 License. For more information, see https://creativecommons.org/licenses/by/4.0/

This article has been accepted for publication in a future issue of this journal, but has not been fully edited. Content may change prior to final publication. Citation information: DOI 10.1109/ACCESS.2021.3135707, IEEE Access

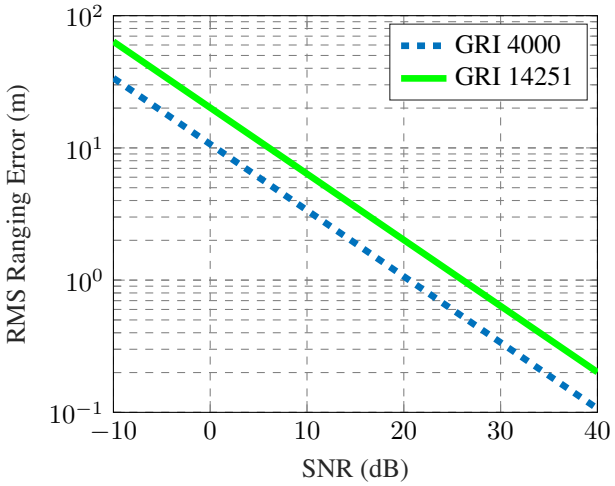

FIGURE 1: Showing the influence of GRI and SNR on the pseudorange error.

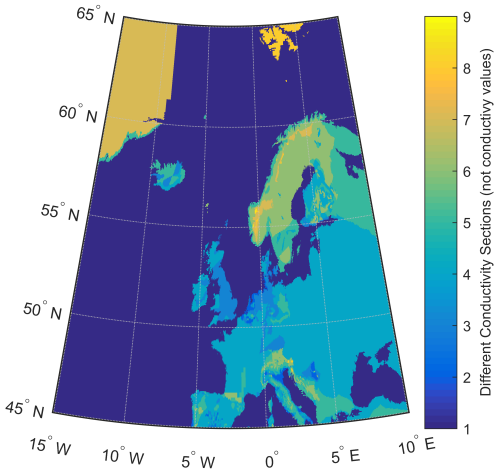

FIGURE 3: Showing different conductivity segments in European eLoran coverage area.

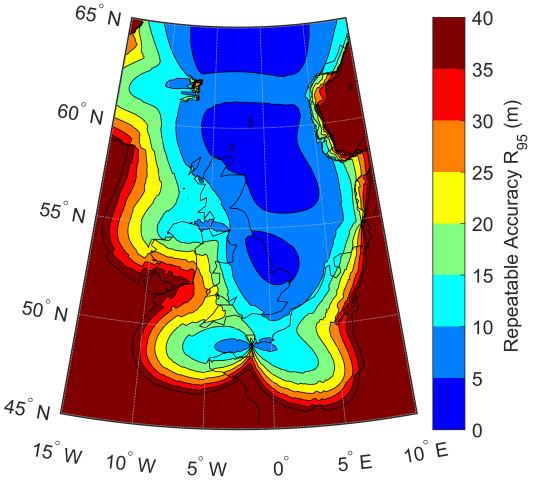

FIGURE 2: Repeatable accuracy plot. DLoran is assumed to be everywhere in the coverage area.

the geographical area. This assumption suggests that each grid point in the coverage area is a port or harbour, which is unrealistic and uneconomical. Therefore, this work aims to model realism by using the long and short term ASF variations to dilute the effects of dLoran in regions that are not harbours and ports. The following section describes our proposed model.

III. PROPOSED ACCURACY MODEL

This section starts by summarising the long term ASF variation model we developed in our previous work [20], [29] and then goes on to describe the short term ASF variation model to enhance the accuracy model used for eLoran service volume coverage prediction.

LONG TERM ASF VARIATION MODEL

This model takes into account the contribution of the long term ASF variations on eLoran transmitter ranging error. The eLoran propagation path is a mixture of seawater and land paths. The receiver-transmitter land path distances are determined using the conductivity data provided by ITU. Fig. 3 shows different ground conductivity segments across Europe represented by numbers ranging from 1 to 9. The number 1 here represents seawater conductivity, while other numbers represent different terrain conductivities. We found that more than 70% of the coverage regions have the same conductivity values. The United Kingdom and Ireland also have more than 70% of similar conductivity values. Because of this, we assumed a direct correlation between the land path distance and ASF variations. This assumption is consistent with the results obtained by the same study conducted in the US [37]. The eLoran temporal ASF data of four eLoran stations Lessay, Anthorn, Soustons and Sylt, was measured at the Harwich, UK reference station from October 2009 to October 2010. We then determined the land path distance from the transmitter to the reference station. We fitted the yearly ASF variations of the transmitters, transmitter powers, and land path distances into a proposed model given by Equation (4).

$$\sigma_l = \left[\alpha \left(\frac{P}{P_0} \right)^{1/2} \exp(\beta D) \right] \tag{4}$$

where D represents the land path distance in km, P is the power transmitted in kW, P_0 is the highest transmission power of all the coverage transmitters, while α and β are derived from the model. The coefficients of the proposed model were found to be $\alpha = 0.17$ m and $\beta = 0.0106$ km^{-1}. The square of equation (4) is represented by $\sigma^2_{LT_{ASF}}$ throughout this paper. We use the error propagation laws to

This work is licensed under a Creative Commons Attribution 4.0 License. For more information, see https://creativecommons.org/licenses/by/4.0/

This article has been accepted for publication in a future issue of this journal, but has not been fully edited. Content may change prior to final publication. Citation information: DOI 10.1109/ACCESS.2021.3135707, IEEE Access

state the TOA variance in the following form

$$\sigma^2_{TX} = \sigma^2_{Noise} + \sigma^2_{LT_{ASF}} + \sigma^2_{ST_{ASF}} + \sigma^2_{Other} \quad (5)$$

where σ^2_{Noise}, $\sigma^2_{LT_{ASF}}$ and $\sigma^2_{ST_{ASF}}$ are the TOA variances due atmospheric noise, long term ASF and short term ASF variations respectively. The term σ^2_{Other} represents the TOA variance due to other error sources and is considered to be negligible in this study.

$$\sigma^2_{Noise} = L_m \frac{337.5^2}{N_a \gamma} \quad (6)$$

Substituting equation (3) into (6) gives

$$\sigma^2_{Noise} = K_m \frac{GRI}{(1 - L_b) \cdot \gamma} \quad (7)$$

where K_m is a constant equals to $\frac{L_m \times 337.5^2}{8 \times 10^5}$. Equation (7) suggests that longer GRIs increases the TOA variance. Depending on the value of the horizontal dilution of precision, the position accuracy may become large. Good position errors is obtained when the receiver selects the lower GRI transmitters in the position solution. The TOA variance, σ^2_{TX}, in regions not designated as reference stations when only σ^2_{Noise} and $\sigma^2_{LT_{ASF}}$ are considered is given by

$$\sigma^2_{TX} = K_m \frac{GRI}{(1 - L_b) \cdot \gamma} + \alpha^2 (\frac{P}{P_0}) \exp(2\beta D) \quad (8)$$

The pseudorange error is the square root of the TOA variance and is given by

$$\sigma_{TX} = \sqrt{K_m \frac{GRI}{(1 - L_b) \cdot \gamma} + \alpha^2 (\frac{P}{P_0}) \exp(2\beta D)} \quad (9)$$

This study assumes that ASF corrections remain valid at a 50 km radial distance from the reference station. This assumption was verified using the results from the eLoran trials held at Harwich, United Kingdom. The TOA variance is given by

$$\sigma^2_{TX} = \begin{cases} K_m \frac{GRI}{(1-L_b)\cdot\gamma} & d \leq 50km, \\ K_m \frac{GRI}{(1-L_b)\cdot\gamma} + \alpha^2 (\frac{P}{P_0}) \exp(2\beta D) & d > 50km \end{cases} \quad (10)$$

Equation (10) shows the blanking loss, land path and GRI influence on the pseudorange error. The results depicted in fig. 1 suggest that a pseudo-range error increases with increasing GRI and decreases with an increase in the SNR. Fig. 4 indicate that a decreasing SNR and an increase in the land path distance leads to an exponential growth in the pseudorange error.

SHORT TERM ASF VARIATION MODEL

The literature [25], [38]–[41] proposes that the atmospheric refractive index at any grid point is given by

$$\eta = 1.0 + \left[\underbrace{77.6 \frac{P}{T}}_{dry-term} + \underbrace{3730 \frac{e_s \cdot RH}{T^2}}_{wet-term} \right] \times 10^{-6} \quad (11)$$

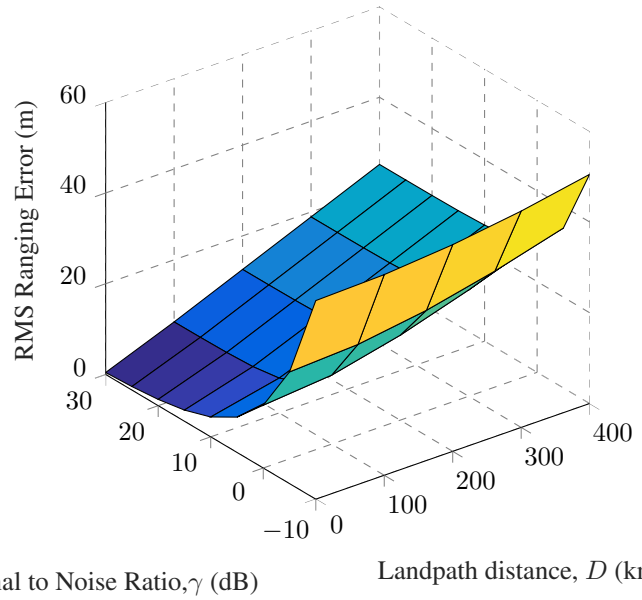

FIGURE 4: The influence of SNR and Landpath distance on the pseudo range error for GRI 6731. The integration time is assumed to be $T_i \approx 5$ while L_b and K_m are set at 0.83 and 0.7 respectively.

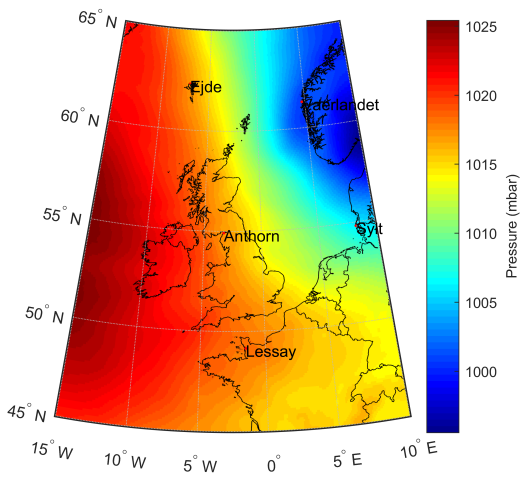

FIGURE 5: Showing Atmospheric Pressure levels experienced in the coverage area. The coverage results suggest that the Atlantic Ocean experiences high pressure levels compared to other areas.

Wenzel et al. [22] proposed that the wet term of the refractive index is insignificant and that it is sufficient to model the dry term only. Equation (11) reduces to

$$\eta = 1.0 + 77.6 \frac{P}{T} \times 10^{-6} \quad (12)$$

where P is the pressure and T is the temperature. Our short term ASF model uses temperature and pressure information for a yearly period from October 2009 to October 2010. The dataset used was extracted from the European Centre for Medium-Range Weather Forecasting (ECMWF) ERA-

This work is licensed under a Creative Commons Attribution 4.0 License. For more information, see https://creativecommons.org/licenses/by/4.0/

This article has been accepted for publication in a future issue of this journal, but has not been fully edited. Content may change prior to final publication. Citation information: DOI 10.1109/ACCESS.2021.3135707, IEEE Access

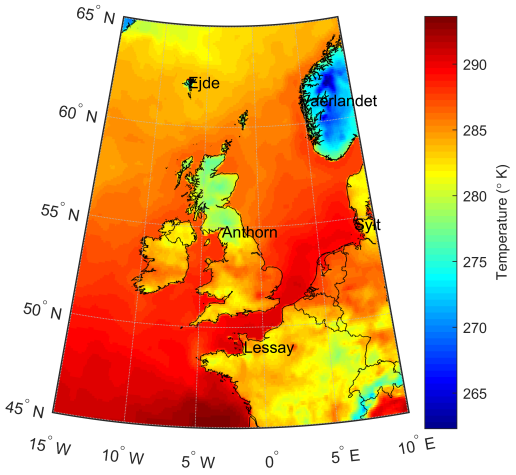

FIGURE 6: Showing temperature levels in the coverage area. The northern part of the UK is colder than the South. The results suggest that the South-East is warmer than anywhere else in the UK and that Norway experiences the lowest temperatures in the region.

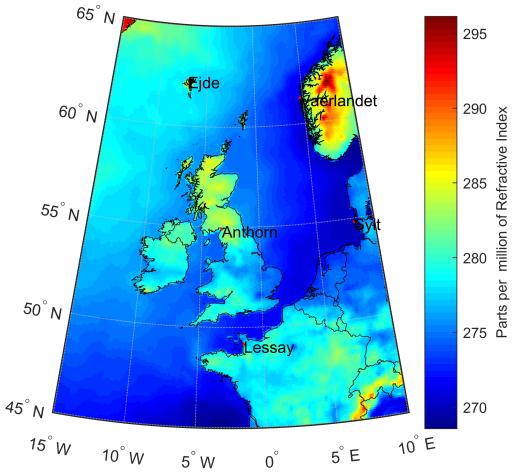

FIGURE 7: Showing atmospheric refractivity experienced in the coverage area.

40 dataset downloaded from the British Atmospheric Data Centre (BADC) [21]. We used a bilinear transformation to interpolate and fit the data into a grid equivalent to the coverage area. Fig. 5 and 6 show pressure and temperature plots over the European eLoran service area. Sea areas experience high temperatures and lower atmospheric pressure compared to other areas.

By definition, the signal propagating in a medium with a refractive index of η travels with a speed equal to c/η. The speed of a Loran signal propagating through the air space, PF, is given by

$$PF = \frac{d}{c/\eta} = \frac{d}{c} \cdot \eta \tag{13}$$

where d is the propagation distance, c is the speed of light in

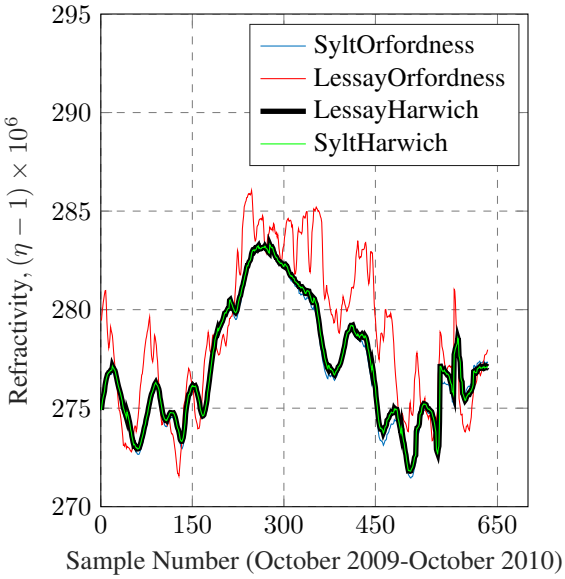

FIGURE 8: Shows refractivity of the received signals at Harwich and Orfordness. Harwich and Orfordness are 25.8 km apart. The curves demonstrate that the values of the refractivity at the locations throughout the year are closely correlated. However, there is more decorrelation of the Lessay signal at Orfordness compared to other signals.

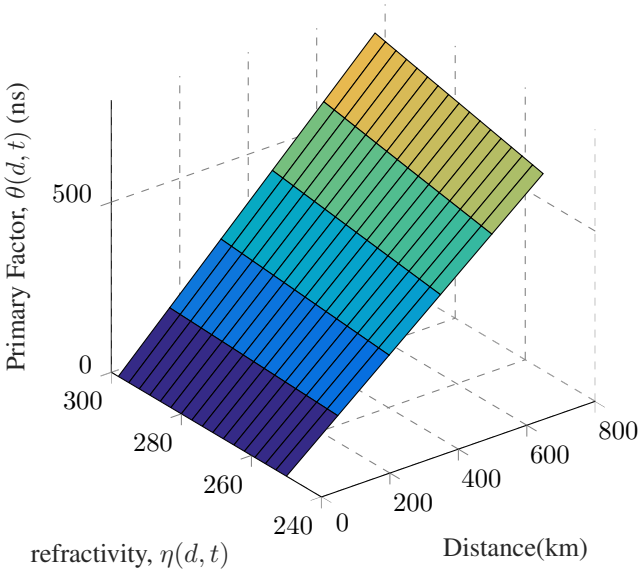

FIGURE 9: Shows primary factor delay performance, $\theta(d,t)$ of the received signal at a distance, d from the transmitter. This primary factor delay is determined using refractivity given by $\eta(d,t)$.

This work is licensed under a Creative Commons Attribution 4.0 License. For more information, see https://creativecommons.org/licenses/by/4.0/

This article has been accepted for publication in a future issue of this journal, but has not been fully edited. Content may change prior to final publication. Citation information: DOI 10.1109/ACCESS.2021.3135707, IEEE Access

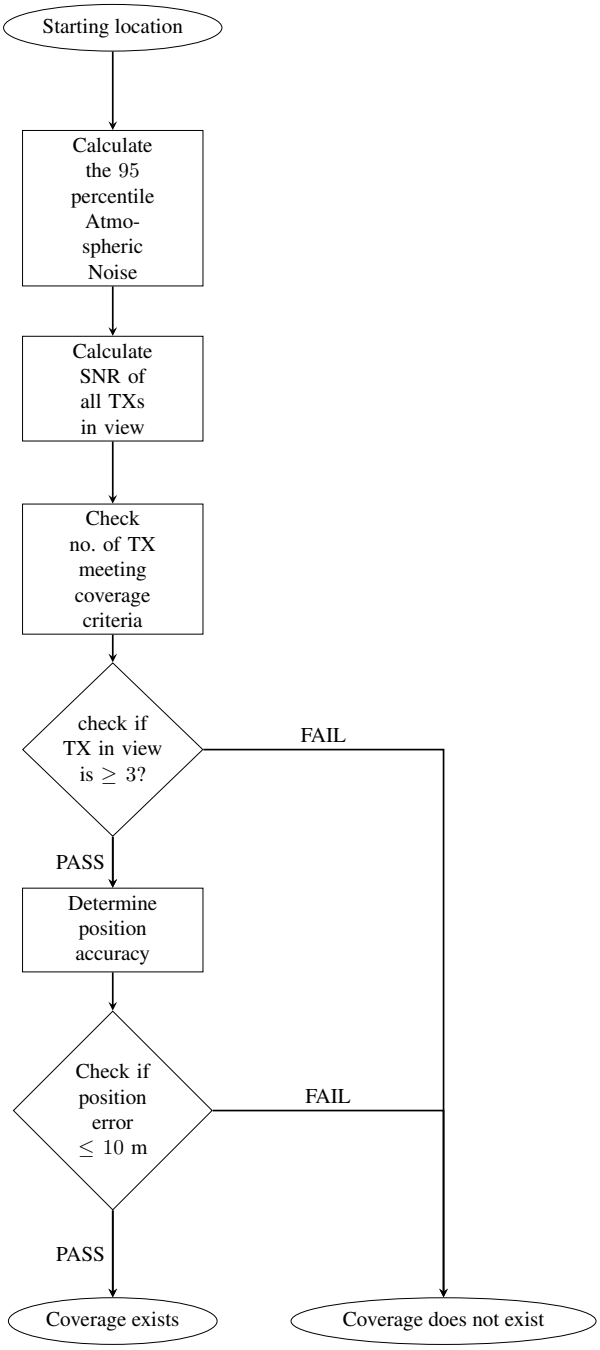

FIGURE 10: Procedure for accuracy calculation.

a vacuum, and η is the refractive index of air. The primary factor expressed in terms of refractivity N is given by

$$PF = \frac{d}{c}(N \times 10^{-6} + 1) \tag{14}$$

This can be rewritten as

$$PF = \frac{d}{c}N \times 10^{-6} + \frac{d}{c} \tag{15}$$

The first part of equation 15 is the propagation delay introduced by the air refractivity, while the second is the propagation time if the medium is vacuum since c is the speed of light in vacuum. The PF variance in square seconds is given by

$$\sigma^2_{PF} = \frac{d^2}{c^2} \cdot (\sigma^2_N \times 10^{-12}) \tag{16}$$

The PF variance in square meters is given by

$$\sigma^2_{PF} = d^2 \cdot (\sigma^2_N \cdot 10^{-12}) \tag{17}$$

where σ_N is the standard deviation of the refractivity of the primary factor delay along the propagation path, and d is the path distance. Equation 17 represents the short ASF variation model ($\sigma^2_{ST_{ASF}}$) and is used to modify the TOA variance model at regions not designated as harbours or ports.

1) Calculation of σ^2_N from the Weather data

This section describes the steps taken to determine σ_N at any grid point.

- Store the daily atmospheric pressure and temperature data for each grid point from October 2009 to October 2010
- Calculate daily Refractivity for each grid point using equation 12.
- Calculate the refractivity variance, σ^2_N for each grid point, using the whole year data.

Fig. 11 shows standard deviation of refractivity. The results suggest that the standard deviation is higher in Norway compared to the rest of Europe.

2) Calculation of σ^2_N along the propagation path

As the signal propagates from the transmitter to the receiver located at a particular grid point, it experiences a variance in the TOA due to changes in the weather parameters. In this study, the steps taken to estimate σ^2_N along the propagation path are as follows

- Divide the propagation path into equal segments
- Load the yearly σ^2_N refractive variance for the whole grid.
- The total σ^2_N experienced by the transmitted signal to the grid point equals the sum of σ^2_N for each segment. This idea is consistent with the propagation of error laws.

Equation (17) represents the contribution of the weather parameters on the transmitter ranging errors. It models TOA variance introduced by weather changes at grid points that are not harbours and ports. A piecewise function shown by equation (19) presents an improved accuracy model, which includes the contribution of atmospheric noise and long and short term variations. This model shows that the pseudo-range error at grid points outside the ports and harbours is worse than when measured at port and harbour locations. The model realism imitates a real eLoran system.

This work is licensed under a Creative Commons Attribution 4.0 License. For more information, see https://creativecommons.org/licenses/by/4.0/

This article has been accepted for publication in a future issue of this journal, but has not been fully edited. Content may change prior to final publication. Citation information: DOI 10.1109/ACCESS.2021.3135707, IEEE Access

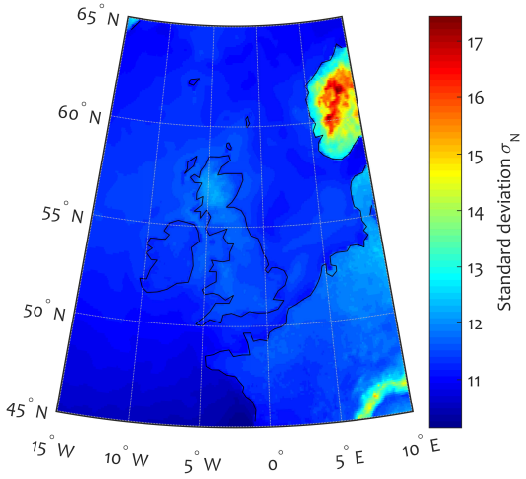

FIGURE 11: Shows the variation of yearly Refractivity from its mean values at all grid points. The minimum value is 9.6, while the maximum value is 17.4. These refractive standard deviation values by the short term ASF model

3) Description of Repeatable Accuracy Calculation Method

The International Maritime Organisation (IMO) [18] stipulates the position error not exceeded 95% of the time. Repeatable accuracy is given by

$$a_{DRMS} = \sigma_{TX} \underbrace{\sqrt{(G_{1,1} + G_{2,2})}}_{\text{HDOP}} \tag{18}$$

The flowchart in fig. 10 summarises repeatable accuracy calculation for eLoran . Before starting repeatable accuracy calculation within the geographical area, we load conductivity, ground field strength, skywave and atmospheric noise data into the coverage software written using MATLAB. The geographical area is divided into equal grid points using a specified grid resolution set to 0.1 in latitude and longitude. At the starting location where repeatable accuracy is measured, the 95 percentile atmospheric noise is estimated, and the SNRs of all the transmitters in view are calculated. Once this is done, the algorithm checks if the transmitters meet SNR criteria $SNR \geq -10$, skywave-groundwave ratio(SGR) criteria. The SGR criteria is stated in [29]. If three or more transmitters meet the SNR and SGR criteria, position accuracy is the determined using algorithm described in [2], [29]. Repeatable accuracy cannot be determined when less than three transmitters meet coverage criteria because three or more are needed to perform geolocation. After three or more transmitters meet the coverage criteria, the algorithm checks if the resulting position accuracy meets the 10m or less accuracy set by IMO for HEA manoeuvres. The receiver's location is out of coverage if it does not meet IMO accuracy requirements. Otherwise, it is said to be in coverage.

COMBINED LONG TERM AND SHORT ASF VARIATION MODEL

The proposed accuracy model includes the long-term and short term ASF variations under the following assumptions

- Similar ground conductivity variations are experienced everywhere in the geographical area.
- The long-term ASF variations increase with increasing Land path distances.
- The short-term ASF variations are due to the changes in meteorological parameters.
- The pseudorange error due to the skywave signal is insignificant.
- Carrier wave interference influence on the position error is negligible.
- Every port and harbour has a reference station or deploys a dLoran system
- eLoran meets the 10 m accuracy requirement set by the IMO at 50 km radial distances from all ports and harbours.
- The receiver signal processing module can blank out all CRI contaminated pulses.
- The averaging process eliminates transmitter jitter and its effects.
- The European Loran System transmitters are still in operation.

The reason behind these assumptions is to derive a repeatable accuracy model that can be modified as more data becomes available. Sophisticated receiver signal processing techniques minimize the influence of skywave, carrier wave and Cross Rate Interference. However, they can be modelled and represented by σ^2_{Other}. Equation (19) determines the TOA variance at any grid point. If the reference station-grid point distance is less or equal to 50 km, the top part of the piece-wise function shown by equation (19) represents the signal TOA variance; otherwise, the lower part, which includes long and short term ASF models represents the signal TOA variance. For distances less or equal to 50km, we assume that dLoran mitigates the long and short term TOA variance hazards.

$$\sigma^2_{TX} = \begin{cases} L_{impl} \dfrac{337.4^2}{N_a \cdot \gamma} & d \leq 50km, \\ L_{impl} \dfrac{337.4^2}{N_a \cdot \gamma} \cdots & \\ + \left[\alpha^2 \left(\frac{P}{P_0}\right) \cdot \exp\left(2\beta D\right)\right] \cdots & \\ + d^2 \cdot \sigma_N^2 \cdot 10^{-12} & d > 50km \end{cases} \tag{19}$$

The TOA variances of the transmitter are used in the position solution to determine position error or repeatable accuracy using the procedure described by fig. 10.

IV. RESULTS AND DISCUSSION

This section presents the repeatable accuracy results obtained using our developed accuracy model. We first draw the

This work is licensed under a Creative Commons Attribution 4.0 License. For more information, see https://creativecommons.org/licenses/by/4.0/

This article has been accepted for publication in a future issue of this journal, but has not been fully edited. Content may change prior to final publication. Citation information: DOI 10.1109/ACCESS.2021.3135707, IEEE Access

reader's attention to the repeatable accuracy plot shown in fig. 2. The results obtained assume that every grid point has dLoran capability. The contours show accuracy results. It can be seen that the East part of the coverage area has better repeatable accuracy than the West. There are no transmitters in the Republic of Ireland; hence accuracy is poor in the West of the coverage area due to bad HDOP. We noted that this model needed to be modified as it is unrealistic and uneconomical to have every grid point having a reference station.

A. INFLUENCE OF THE LONG TERM VARIATIONS ON RANGING ERRORS

Fig. 12 shows the eLoran repeatable accuracy for the chosen geographical area without differential ASFs. The land path model is essentially used to determine repeatable accuracy at all regions that are not harbours or ports in the coverage area. A comparison between fig. 2 and fig. 12 suggest that the accuracy has become poorer in fig. 12 as expected due to the contribution of the land path model. It is important to note that we have added a component to the TOA variance matrix, resulting in poor repeatable accuracy compared to fig. 2. The best position accuracy of 0-10m in fig. 12 is in some parts of the Atlantic ocean. Repeatable accuracy is above 10m in most parts of the British Isles and the Atlantic ocean. The results show that none of the areas in the British Isles meets the IMO accuracy requirements. The next step is to include the results for grid points hosting reference stations. The plot in fig.12 is a good representation of the coverage elsewhere except at the SOLAS ports and harbours.

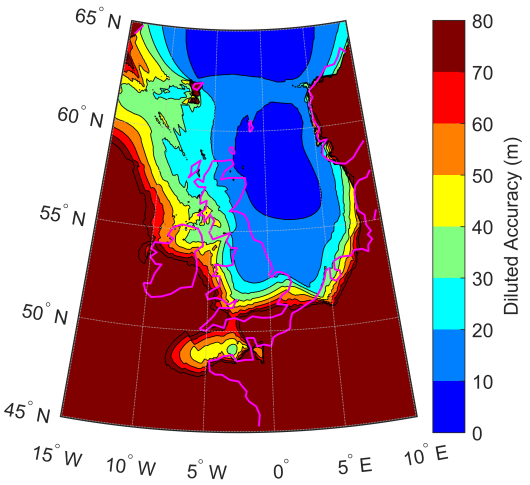

FIGURE 12: Accuracy plot modified everywhere using the Land path model.

1) Modified Accuracy due to Land path Model & dLoran

This section discusses results using Long term ASF model and the reference station coverage prediction model. We obtained from the GLAs the coordinates of places used as harbours and ports where TOA variance is only due to atmospheric noise. The next step of our algorithm is to include dLoran accuracy in the harbour and port designated areas. When using a system with dLoran capability, such regions will have accuracy below 10m as the IMO resolution requires.

It is reasonable to assume that all harbours and ports have reference stations and meet the IMO repeatable accuracy requirement of 10 m at 50 km radial distances. Various eLoran trials conducted up to 100 km from the Harwich harbour in the United Kingdom verified this assumption. The accuracy at port and harbour regions is factored into the accuracy plot to make it more realistic. Fig. 13 shows the repeatable accuracy modified by the land path model at other regions in the coverage area except at harbours and ports. The dark blue circles represent the accuracy performance at port regions in the coverage area. Fig. 13 demonstrates a much-improved accuracy model which is realistic than the one shown in [2]. This plot shows that IMO accuracy requirements are met at reference station locations and some parts of the Atlantic Ocean. Repeatable accuracy is poor in the west of the British Isles, Irish sea and the Republic of Ireland because of poor transmitter geometry. This model ignored the weather effects on repeatable accuracy. The following section discusses the results of the short term variation in the TOA variance model.

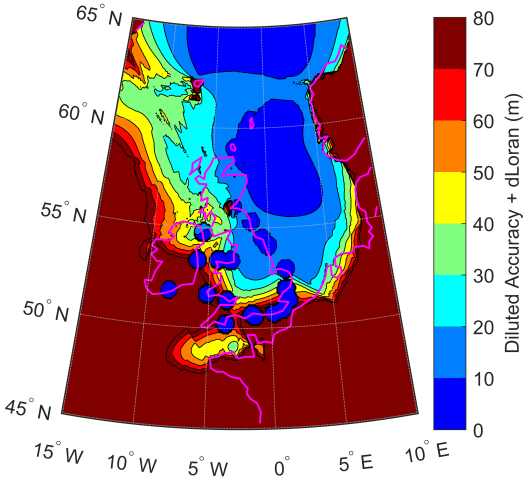

FIGURE 13: Shows repeatable accuracy plot after including the long-term ASF variations outside port regions while meeting a 10m IMO requirement at all harbours.

B. INFLUENCE OF THE SHORT TERM VARIATIONS ON RANGING ERRORS

Repeatable accuracy varies temporally and spatially in the coverage area due to changes in the weather parameters. DLoran can only correct the effect of these changes at locations within the harbour's ASF correction spatial decorrelation limits. Beyond this, the position error is unmitigated due to limited dLoran resources.

This work is licensed under a Creative Commons Attribution 4.0 License. For more information, see https://creativecommons.org/licenses/by/4.0/

This article has been accepted for publication in a future issue of this journal, but has not been fully edited. Content may change prior to final publication. Citation information: DOI 10.1109/ACCESS.2021.3135707, IEEE Access

1) Modified Accuracy due to changes in Meteorological Parameters

The accuracy plot in fig. 13 is made more realistic by including the effects of the changes in meteorological parameters at all areas except at ports and harbours. The results shown in Fig. 14 show that positioning accuracy in the other areas except SOLAS ports is worse compared to fig. 13. The coverage plot also shows better coverage in the North Sea than in the Irish sea. The results suggest that the IMO accuracy requirement are only met at harbours and ports. The results are consistent with those obtained by the GLAs during eLoran trials. Poor repeatable accuracy in the Irish Sea and some parts of Ireland is due to poor transmitter geometry. Installation of at least two transmitters in Ireland is needed to enhance transmitter geometry. The added transmitters are likely to improve the accuracy plot in the region between the Irish Sea and the British Isles. Fig. 14 portrays a real eLoran system.

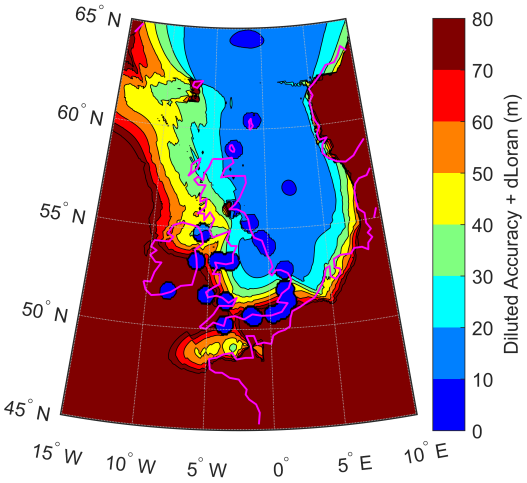

FIGURE 14: Accuracy plot showing the contribution of the long term and short term ASF variations.

V. CONCLUSIONS

This paper has presented a realistic eLoran accuracy model for HEA. The results have demonstrated that the short term ASF variations significantly contribute to the positioning error and must be included in the accuracy model. The results indicate that eLoran can achieve a 20 m accuracy or better in the North Sea, while a 10 m accuracy would be achievable at the SOLAS ports if eLoran was reintroduced in Europe. The results also show that eLoran meets navigational requirements for HEA. Nevertheless, the repeatable accuracy around the Irish sea exceeds 80 m and does not meet marine navigation requirements compared to GPS. Coverage can be enhanced by including at least two eLoran transmitters in Ireland.

REFERENCES

[1] Carroll, James V. "Vulnerability assessment of the US transportation infrastructure that relies on the global positioning system." The Journal of Navigation 56.2 (2003): 185-193.

[2] Safar, Jan, Caspar K. Lebekwe, and Paul Williams. "Accuracy Performance of eLORAN for Maritime Applications." Annual of Navigation (2010): 109-121.

[3] Johnson, Gregory, Ruslan Shalaev, Richard Hartnett, Peter Swaszek, and Mitch Narins. "Can Loran meet GPS backup requirements?" *IEEE Aerospace and Electronic Systems Magazine* 20.2 (2005): 3-12.

[4] Johnson, G., R. Hartnett, P. Swaszek, Keith Gross, C. Oates, and M. Narins. "FAA Loran-C Propagation Studies." *In Annual Technical Meeting, Institute of Navigation, Anaheim, CA*, pp. 22-24. 2003.

[5] Swaszek, Peter F., Richard J. Hartnett, Gordon Weeks, Gregory W. Johnson, and Christian Oates.*A Demonstration of High Accuracy Loran-C for Harbor Entrance and Approach Areas*. US Coast Guard Academy, Center for Advanced Studies, 2003.

[6] Boyce, CO Lee. "Atmospheric noise mitigation for LORAN." PhD diss., Stanford University, 2007.

[7] Safar, Jan, F. Vejrazka, and Paul Williams. "Assessing the limits of eLoran positioning accuracy." *TransNav, International Journal on Marine Navigation and Safety od Sea Transportation* 5.1 (2011).

[8] Hargreaves, C., P. Williams, and M. Bransby. "ASF quality assurance for eLoran." *Position Location and Navigation Symposium (PLANS), 2012 IEEE/ION*. IEEE, 2012.

[9] Van Willigen, Durk, Rene Kellenbach, Cees Dekker, and Wim van Buuren. "eDLoran-next generation of differential Loran." *In Proceedings of the European Navigation Conference*, pp. 15-17. 2014.

[10] Offermans, G. W. A., A. W. S. Helwig, and D. Van Willigen. "The eurofix datalink concept: reliable data transmission using Loran-C." In *Proceedings of the 25th Annual Technical Symposium of the International Loran Association*, pp. 3-7. 1996.

[11] Carroll, K., Anthony Hawes, Benjamin Peterson, Kenneth Dykstra, Peter Swaszek, and Sherman Lo. "Differential Loran-C." In *Proceedings of GNSS 2004-The European Navigation Conference*. 2004.

[12] Johnson, Gregory W., Peter F. Swaszek, Richard J. Hartnett, Ken Dykstra, Ruslan Shalaev, and Sherman Lo. "Temporal Variation of Loran ASFs and their Effects on HEA Navigation." In Proceedings of the European Navigation Conference ENC2008, Toulouse, France, pp. 22-28. 2008.

[13] Williams, Paul, Sally Basker, and Nick Ward. "e-Navigation and the Case for eLoran." *The Journal of Navigation* 61.3 (2008): 473-484.

[14] Peterson, Benjamin B., C. A. Schue, James M. Boyer, and James R. Betz. "Enhanced LORAN-C data channel project." In *Proceedings of the International Symposium on Integration of LORAN-C/Eurofix and EGNOS/Galileo*, pp. 186-197. 2000.

[15] Lo, Sherman C., Benjamin B. Peterson, and Per K. Enge. "Loran Data Modulation: A Primer [AESS Tutorial IV]." *IEEE Aerospace and Electronic Systems Magazine* 22, no. 9 (2007): 31-51.

[16] Lo, S., Peterson, B., Boyce, C. and Enge, P., 2008, October. Loran coverage availability simulation tool. In *Proceedings of the Royal Institute of Navigation (RIN) NAV08/International Loran Association 37th Annual Meeting* (p. 12).

[17] Safar, Jan. "Analysis, modelling and mitigation of cross-rate interference in enhanced LORAN." (2014).

[18] *Resolution A.1046(27), World Wide Radionavigation System*, December 2011.

[19] Last, David, and Y. Bian. "Carrier wave interference and Loran-C receiver performance." In IEE Proceedings F (Radar and Signal Processing), vol. 140, no. 5, pp. 273-283. IET Digital Library, 1993.

[20] Lebekwe, Caspar K., Abid Yahya, and Ivan Astin. "An Improved Accuracy Model Employing an e-Navigation System." In 2018 9th IEEE Annual Ubiquitous Computing, Electronics & Mobile Communication Conference (UEMCON), pp. 152-158. IEEE, 2018.

[21] https://nerc.ukri.org/research/sites/data/

[22] Robert Wenzel, Peter Morris, and Kirk Montgomery. An Examination of Loran Signal Propagation Temporal Variation Modeling, Proceedings of the International Loran Association 35th Annual Meeting, Groton, CT, October 2006.

[23] Lo, Sherman, Lee Boyce, Per Enge, Ben Peterson, Bob Wenzel, Peter Morris, and K. Carroll. "Loran for RNP 0.3 Approach: The Preliminary Conclusions of Loran Integrity Performance Panel (LORIPP)." In Proceedings of the 16th International Technical Meeting of the Satellite Division of The Institute of Navigation (ION GPS/GNSS 2003), pp. 877-888. 2003.

This work is licensed under a Creative Commons Attribution 4.0 License. For more information, see https://creativecommons.org/licenses/by/4.0/

This article has been accepted for publication in a future issue of this journal, but has not been fully edited. Content may change prior to final publication. Citation information: DOI 10.1109/ACCESS.2021.3135707, IEEE Access

[24] Safar, Jan, F. Vejrazka, and Paul Williams. "Assessing the limits of eLoran positioning accuracy." TransNav, International Journal on Marine Navigation and Safety od Sea Transportation 5, no. 1 (2011).
[25] Y. Pu, X. Zheng, D. Wang and X. Xi, "Accuracy Improvement Model for Predicting Propagation Delay of Loran-C Signal Over a Long Distance," in IEEE Antennas and Wireless Propagation Letters, vol. 20, no. 4, pp. 582-586, April 2021, doi: 10.1109/LAWP.2021.3057942.
[26] C. Hargreaves, P. Williams, J. Safar and M. Bransby, "Radio-navigation system coverage modelling software," 2015 International Association of Institutes of Navigation World Congress (IAIN), 2015, pp. 1-7, doi: 10.1109/IAIN.2015.7352222.
[27] Y. Hongjuan, W. Lili, P. Yurong and X. Xiaoli, "Analysis of diurnal variation on long-wave ground wave propagation delay," 2017 Sixth Asia-Pacific Conference on Antennas and Propagation (APCAP), 2017, pp. 1-3, doi: 10.1109/APCAP.2017.8420742.
[28] Johnson, Gregory, Peter Swaszek, Jan-Hendrik Oltmann, and Michael Hoppe. "Feasibility Study of R-Mode combining MF DGNSS, AIS, and eLoran Transmissions."
[29] Lebekwe, Caspar, and Ivan Astin. "ELoran Service Volume Coverage Prediction." PhD diss., University of Bath, 2018.
[30] Lo, Sherman, and Per Enge. "Analysis of the Effects of ASF Variations for Loran RNP 0.3." In Proceedings of the 32nd Annual International Loran Association Meeting. 2003.
[31] Lo, Sherman C., Robert Wenzel, Greg Johnson, and Per K. Enge. "Assessment of the methodology for bounding Loran temporal ASF for aviation." In Proceedings of the 2008 National Technical Meeting of the Institute of Navigation, pp. 432-442. 2008.
[32] B. Parkinson, J. Doherty, J. Darrah, A. Donahue, L. Hirsch, D. Jewell, D. W. Klepczynski, J. Levine, K. Lewis, E. Stear, P. Ward, and P. Rambow, "Independent Assessment Team (IAT) Summary of Initial Findings on eLoran," tech. rep., Institute for Defense Analyses, 2009.
[33] John A. Volpe National Transportation System Center, Vulnerability Assessment of the Transportation Infrastructure Relying on the Global Positioning System, 2001
[34] P. Williams, C. Hargreaves, D. Last, and N. Ward, "eLoran in the UK: Leading the Way," in Proceedings of the ION PaciïňĄc PNT Conference, April 2013.
[35] Lo, Sherman, Robert Wenzel, and Per Enge. "Analysis and Modeling of Skywave Behavior." (2009).
[36] Zhao, Zhenzhu, Jiangfan Liu, Jinsheng Zhang, and Xiaoli Xi. "Sky-ground wave signal separation in enhanced Loran based on Levenberg-Marquart algorithm." IET Radar, Sonar & Navigation (2021).
[37] FAA (AND-700) report to DOT. An Analysis of Loran-C Performance, its Suitability for Aviation Use, and Potential System Enhancements,. July 2002.
[38] K.E. Ukhurebor, S.O. Azi "Review of methodology to obtain parameters for radio wave propagation at low altitudes from meteorological data: new results for Auchi area in Edo State, Nigeria" J. King Saud Univ. - Sci., 31 (4) (2019), pp. 1445-1451, doi.org/10.1016/j.jksus.2018.03.001
[39] K.E. Ukhurebor, S.O. Azi, U.O. Aigbe, R.B. Onyancha, J.O. Emegha, "Analyzing the uncertainties between reanalysis meteorological data and ground measured meteorological data" Measurement, vol. 165, 2020. doi.org/10.1016/j.measurement.2020.108110
[40] Agbo, E.P., Ettah, E.B. & Eno, E.E. The impacts of meteorological parameters on the seasonal, monthly, and annual variation of radio refractivity. Indian J Phys 95, 195-207 (2021). https://doi.org/10.1007/s12648-020-01711-9
[41] Alimgeer KS, Awas M, Ijaz B, Khan SA, Subhan F, Ahmad N (2018) Statistical estimation and mathematical modelling of tropospheric radio refractivity based on meteorological data. Meteorology and Measurement Systems. Vol. 25(1), pp. 115 - 128.

CASPAR K. LEBEKWE (Member, IEEE) was awarded a degree of MEng in Electronics and Communications Engineering at the University of Bath in 2008. He holds a Ph.D. in Electrical and Electronics Engineering, sponsored by the General Lighthouse Authorities at the same University. His Ph.D. project was focused on eLoran Service Volume Coverage Prediction. He is currently a Senior Lecturer at Botswana International University of Science and Technology, where he teaches Optical Communications, Antennas and Propagation, Discrete Mathematics, Telemetry, and Remote Control as well as Electromagnetic Field Theory. He is a registered member of the IEEE.

ADAMU MURTALA ZUNGERU (Senior Member, IEEE) received the B.Eng. Degree from the Federal University of Technology, Minna, Nigeria, the M.Sc. degree from Ahmadu Bello University, Zaria, Nigeria, and the Ph.D. degree from Nottingham University, U.K. He was a Research Fellow with the Massachusetts Institute of Technology (MIT), USA, where he also obtained a Postgraduate Teaching Certificate, in 2014. He is currently serving as a Professor and the Head of the Department of Electrical, Computer, and Telecommunications Engineering, Botswana International University of Science and Technology (BIUST). Before joining BIUST, in 2015, he was a Senior Lecturer and the Head of the Electrical and Electronics Engineering Department, Federal University Oye-Ekiti, Nigeria. He is a Registered Engineer with the Council for The Regulation of Engineering in Nigeria (COREN) and the Association for Computing Machinery (ACM), USA. He is the Inventor of a Termite-hill routing algorithm for wireless sensor networks. He has two of his patent applications registered with the World Intellectual Property Organization (WIPO). He has also authored five academic books and over 60 international research articles in reputable journals, including the IEEE SYSTEMS JOURNAL, the IEEE INTERNET OF THINGS JOURNAL, IEEE ACCESS, JNCA (Elsevier), and others, with over 900 citations and H-index of 14. He is at present serving as an Associate Editor to IEEE Access and has also served as an International Reviewer of the IEEE TRANSACTIONS ON INDUSTRIAL INFORMATICS, the IEEE SENSORS, IEEE ACCESS, the IEEE TRANSACTIONS ON MOBILE COMPUTING, the IEEE TRANSACTIONS ON SUSTAINABLE COMPUTING, JNCA (Elsevier), and numerous others. He has also served as the Chairman of the IEEE Botswana Sub-Section (2019-2020), and as the IEEE Region 8 Vitality and Development Subcommittee Member.

IVAN ASTIN (Member, IEEE) gained a BSc in mathematics at the University of Nottingham, before completing an MSc in statistics and PhD in ionospheric physics at the University College of Wales, Aberystwyth. After these, he was a postdoctoral research associate at NERC's Mesosphere-Stratosphere-Troposphere (MST) radar facility, near Aberystwyth.

This work is licensed under a Creative Commons Attribution 4.0 License. For more information, see https://creativecommons.org/licenses/by/4.0/